Decentralized Stability Conditions in DC Microgrids

Khaled Laib, Jeremy Watson, Yemi Ojo and Ioannis Lestas

***Abstract*— We consider the problem of ensuring stability in a DC microgrid by means of decentralized conditions. Such conditions are derived which are formulated as input-output properties of locally defined subsystems. These follow from various decompositions of the microgrid and corresponding properties of the resulting representations. It is shown that these stability conditions can be combined together by means of appropriate homotopy arguments, thus reducing the conservatism relative to more conventional decentralized approaches that often rely on a passivation of the bus dynamics. Examples are presented to demonstrate the applicability and the efficiency of the results derived.**

I. Introduction

The increasing integration of renewable energy in recent years has strengthened the interest in microgrids. Compared to AC microgrids, DC microgrids have been recognized as a natural and simple solution to integrate renewable energy, see [1]. For instance, DC microgrids allow connecting DC components directly for a simple integration of renewable generation devices and storage units. Moreover, in addition to being compatible with modern consumer loads, DC microgrids allow to reduce unnecessary power conversion losses. Thus, DC microgrids have become an attractive option not only for providing support to remote communities, but in many other applications: mobile grids on ships, aircrafts, trains, *etc*., see [2].

A DC microgrid is a power network that consists of small subsystems or buses (generation units, storage units, flexible loads, *etc*.) interconnected via power lines. As each subsystem is usually designed to operate in stand-alone conditions, interconnecting the different buses together may decrease the overall performance and it may even lead to the microgrid instability. Another factor that may lead to network instability is the load type. Briefly speaking, in contrast to constant impedance loads and constant current loads, which normally do not induce stability degradation, constant power loads can lead to network instability due to their negative impedance characteristics.

To establish network wide stability results, existing results [3]–[7] often consider specific cases ranging from neglecting the power line dynamics and considering them purely resistive to considering specific type of loads which do not have a destabilizing effect such as constant impedance and/or constant current loads. Moreover, even in the presence of ZIP loads, assumptions on the amount of constant impedance and constant power loads present are often imposed to guarantee the passivity of the bus dynamics and deduce thus stability of the microgrid. Therefore, new approaches that can reduce the conservatism in the analysis are of high relevance in the analysis of DC microgrids.

In this paper, we focus on the derivation of decentralized conditions through which asymptotic stability of the DC microgrid can be established. The analysis is carried out on models that allow higher order dynamics for the buses (with general loads) and the lines connecting them.

The microgrid representation plays a central role in this paper as the notion of a subsystem is not unique. In particular, any derived stability conditions are inevitably going to be only sufficient when these are decentralized. Therefore, different representations of what constitutes a subsystem can lead to stability results with varying conservatism. Analogous to our previous paper [8] on AC grids, we consider various decompositions for the microgrid including ones that take into account the interconnections with neighbouring buses. Using these representations we present different decentralized conditions for stability (passivity, small gain, *etc*.), which are formulated as input/output conditions on locally defined subsystems. A main contribution of this paper is to show that these conditions derived from different decompositions can be combined using appropriate homotopy arguments thus reducing the conservatism in the analysis.

The paper is structured as follows. Section II presents some graph theory elements, the DC microgrid model and the problem setting. Section III presents the main results of the paper while Section IV presents numerical examples. Conclusions are drawn in Section V.

A. Symbols and notations

The sets of real and complex numbers are denoted by $\mathbf{R}$ and $\mathbf{C}$ respectively. The extended real line $[-\infty, +\infty]$ is denoted $\overline{\mathbf{R}}$ and $\overline{\mathbf{R}}_+$ is the set of real positive numbers including 0 and $+\infty$. The imaginary axis is denoted by $\mathbf{j}\overline{\mathbf{R}}$ where $\mathbf{j} = \sqrt{-1}$. The right half-plane including the imaginary axis is denoted by $\mathbf{C}_+$ and its closure is denoted by $\overline{\mathbf{C}}_+$. The set $\mathbb{RH}_\infty^{p\times q}$ is the set of $p \times q$ real rational transfer functions without poles in $\overline{\mathbf{C}}_+$. For a matrix $F \in \mathbf{C}^{n\times n}$ its transpose and conjugate transpose are denoted by F^T and F^* respectively. The identity matrix is denoted by I and its dimensions are deduced from the context. The Kronecker product of two matrices F_i and F_j is denoted by $F_i \otimes F_j$. The direct sum of matrices F_i with $i = 1, \ldots, n$ is denoted by $\oplus_{i=1}^n F_i$. Finally, in order to ease the notation, for matrices $X, \Pi_{11}, \Pi_{12}, \Pi_{22}$ with compatible dimensions and $\epsilon \geq 0$, we

This work was supported by ERC starting grant 679774.

Khaled Laib, Jeremy Watson, Yemi Ojo and Ioannis Lestas are with the Department of Engineering, University of Cambridge, Cambridge CB2 1PZ, United Kingdom. Emails: <kl507,jdw69,yo259,icl20>@cam.ac.uk

use $X \in \mathbf{QC}(\Pi, \epsilon)$, with $\Pi = \begin{pmatrix} \Pi_{11} & \Pi_{12} \\ \Pi_{12}^* & \Pi_{22} \end{pmatrix}$, to denote

$$\begin{pmatrix} X \\ I \end{pmatrix}^* \quad \Pi \quad \begin{pmatrix} X \\ I \end{pmatrix} \geq \epsilon X^* X \tag{1}$$

and $X \in \overline{\mathbf{QC}}(\Pi, \bar{\epsilon})$ to denote

$$\begin{pmatrix} I \\ -X \end{pmatrix}^* \quad \Pi \quad \begin{pmatrix} I \\ -X \end{pmatrix} \leq -\bar{\epsilon} I.$$

II. Network models and problem setting

A. Algebraic graph theory and microgrid signals

The microgrid is a power system comprised of n_b buses and n_ℓ power lines. We assume that each bus includes a DC-DC converter with its controller and load.

We represent this microgrid as a connected graph $(\mathcal{N}, \mathcal{E})$ where $\mathcal{N} = \{1, 2, \ldots, n_b\}$ is the set of nodes (buses) and $\mathcal{E} = \{1, \ldots, n_\ell\} \subseteq \mathcal{N} \times \mathcal{N}$ is the set of edges (lines). A direction is assigned to each edge which can be arbitrarily chosen. The corresponding $n_b \times n_\ell$ incidence matrix is denoted by $\mathcal{A}$ and it is given by

$$\mathcal{A}_{jk} = \begin{cases} +1 & \text{if edge } k \text{ leaves bus } j, \\ -1 & \text{if edge } k \text{ enters bus } j, \\ 0 & \text{otherwise.} \end{cases}$$

For each node $j \in \mathcal{N}$, the set $\mathcal{E}_j = \{k \in \mathcal{E} : \mathcal{A}_{jk} \neq 0\}$ is the set of edges connected to node j.

Given the aforementioned microgrid settings, we define the following signals.

- The input current at bus j is denoted by $i_j(t)$ and its voltage is denoted by $v_j(t)$.
- The current through line k is denoted by $i_{\ell_k}(t)$ (this denotes the current with the same direction as that of the edge k).
- The vector of all bus voltages and the vector of all line currents are denoted by $V(t) = (v_j(t))_{j \in \mathcal{N}}$ and $I(t) = (i_{\ell_k}(t))_{k \in \mathcal{E}}$ respectively.

B. Line dynamics

We model the power lines as RL components. By applying Kirchoff's voltage law on the k^{th} power line ℓ_k, with $k \in \mathcal{E}$, we obtain

$$\frac{\mathrm{d}i_{\ell_k}(t)}{\mathrm{d}t} = \frac{-r_k}{l_k} i_{\ell_k}(t) + \frac{1}{l_k} \delta V_{\ell_k}(t) \tag{2}$$

where $r_k > 0$ and $l_k > 0$ are the resistance and the inductance of k^{th} line and $\delta V_{\ell_k}(t)$ is the voltage difference across line ℓ_k.

C. Bus dynamics

We consider now a general bus model to account for a broad class of DC-DC converters, controllers and loads.

DC-DC converters (buck, boost, buck-boost, SEPIC, *etc.*) are composed of three main stages: DC stage (battery stage), switching stage and DC output stage (output voltage stage). Some assumptions are usually made in the literature to derive simpler models that can be used for control design.

Assumption 1 *The DC stage is equipped with sufficient energy reserves and the switching is performed at a frequency much higher than the natural frequencies of the converter. Furthermore, the power generated on the battery stage is transferred to the output voltage stage without switching losses.*

Under Assumption 1, it is possible to use an averaged converter model to design controllers satisfying appropriate requirements: output voltage regulation, load sharing, *etc.*.

We consider that each converter is already equipped with its controller and is connected to its load. The converter dynamics as well as the controller dynamics vary depending on the DC microgrid voltage level (low, medium and high), model complexity, control strategy, *etc.*. Therefore, the converter and the controller dynamics will be kept in a general representation for analysis and particular implementations will be discussed in the examples of Section IV. For the load, we consider a general ZIP load model which includes constant impedance, constant current and constant power loads.

A general form of the j^{th} bus dynamics can be described as single input single output dynamical system with $i_j(t)$ as input and $v_j(t)$ as output. These dynamics are represented as follows

$$\begin{cases} \dfrac{\mathrm{d}x_j(t)}{\mathrm{d}t} = f_j\big(x_j(t), i_j(t)\big) \\ v_j(t) = g_j\big(x_j(t), i_j(t)\big) \end{cases} \tag{3}$$

where $x_j(t) \in \mathbf{R}^{n_{x_j}}$ is the state vector at each bus (includes converter, controller, and load states), f_j and g_j are functions of the form $f_j : \mathbf{R}^{n_{x_j}} \times \mathbf{R} \to \mathbf{R}^{n_{x_j}}$ and $g_j : \mathbf{R}^{n_{x_j}} \times \mathbf{R} \to \mathbf{R}$.

D. Microgrid small-signal model

The bus model (3) is in general nonlinear due to the converter and load dynamics even when considering linear controllers; hence the microgrid model is also nonlinear. Equilibrium points can be found by setting the time derivatives in (2)-(3) to zero and then solving the resulting system of equations. Thereafter, a linearization can be performed using an obtained equilibrium. For this purpose, we require the following assumption.

Assumption 2 *The system* (2)-(3) *admits an equilibrium. Moreover, the vector functions f_j and the functions g_j in* (3) *are Lipschitz around the considered equilibrium of* (2)-(3)*.*

Under Assumption 2, the system (2)-(3) can be linearized about the equilibrium being considered. In order to analyze this linearization, let $\overline{q}(t) = q(t) - q|_{eq}$ denote the deviation of any quantity $q(t)$ from its equilibrium value. We denote the microgrid equilibrium by $q|_{eq}$ given by

$$q|_{eq} = \Big(\big(I\big)^T, \quad \big(V\big)^T, \quad \big(x_j\big)_{j \in N}^T \Big)^T |_{eq} \tag{4}$$

Furthermore, we assume that the dynamics (3) when linearized are stabilizable and detectable. Finally, we adopt an input-output representation of the small-signal model of microgrid (2)-(3), and we introduce the following two sets of transfer functions:

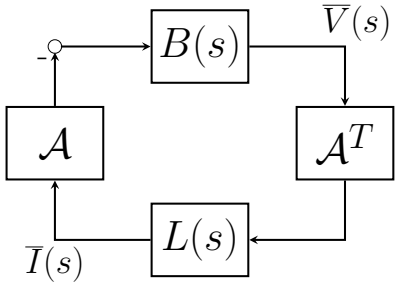

Fig. 1: Block diagram representing the small-signal model (5).

- $L_k(s)$ is the transfer function of the line dynamics (2), from the input $\overline{\delta V_{\ell_k}}(t)$ to the output $\overline{i_{\ell_k}}(t)$;
- $B_j(s)$ is the transfer function of the linearized version of the bus dynamics (3) from the input $\overline{i_j}(t)$ to the output $\overline{v_j}(t)$.

Note that the different $L_k(s)$, obtained from (2), are in $\mathbb{RH}_\infty$ as $-r_k l_k^{-1} < 0$.

We will derive conditions on the frequency response of locally defined subsystems under which stability of the power system (2)-(3) about the equilibrium (4) is guaranteed. To do this, we introduce the following assumption.

Assumption 3 *For each j, $B_j(s) \in \mathbb{RH}_\infty$ with a stabilizable and detectable state-space realization*[1].

Let $\overline{V}(t) = \left(\overline{v_j}(t)\right)_{j\in\mathcal{N}}$ and $\overline{I}(t) = \left(\overline{i_{\ell_k}}(t)\right)_{k\in\mathcal{E}}$; then $\overline{\delta v_{\ell_k}}(t) = (a_k^c)^T\,\overline{V}(t)$ and $\overline{i_j}(t) = -\,a_j^r\;\overline{I_L}(t)$ where a_k^c and a_j^r are the k^{th} column and the j^{th} row of the incidence matrix $\mathcal{A}$ respectively.

The small-signal model of the microgrid (2)-(3) can be represented as a negative feedback interconnection of input-output systems as illustrated in Fig. 1 and is given by

$$\left\{\begin{array}{ll} \overline{V}(s) = -B(s) & \mathcal{A}\;\;\overline{I}(s) \\ \overline{I}(s) = \;\; L(s) & \mathcal{A}^T\;\overline{V}(s) \end{array}\right. \tag{5}$$

with $B(s) = \oplus_{j=1}^{n_b} B_j(s)$ and $L(s) = \oplus_{k=1}^{n_\ell} L_k(s)$ where $B_j(s) \in \mathbb{RH}_\infty$ and $L_k(s) \in \mathbb{RH}_\infty$.

III. Main results

The following theorem gives sufficient conditions for the local asymptotic stability of the equilibrium (4) of the DC microgrid (2)-(3) based on input/output conditions on the subsystems in (5).

Theorem 1 *Under Assumptions 1-3, the equilibrium* (4) *of the power system* (2)-(3) *with its small-signal model* (5) *is locally asymptotically stable if for all $\omega \in \overline{\mathbf{R}}_+$ at least one of the following two statements is satisfied.*

[1]The stabilization and the detectability assumptions ensure that there are no pole/zero cancellations in $\mathbf{C}_+$ in the transfer function.

- **Statement 1:** *For every $j \in \mathcal{N}$, there exist scalars $\gamma_{j1}(\omega) \geq 0$ and $\gamma_{j2}(\omega) \geq 0$ and $\epsilon_{B_j}(\omega) > 0$ such that*

$$\begin{array}{l} B_j(\mathbf{j}\omega) \in \mathbf{QC}\left(\gamma_{j1}(\omega)\Pi_1^{B_j} + \cdots \right. \\ \qquad \left. \cdots + \gamma_{j2}(\omega)\Pi_2^{B_j}(\mathbf{j}\omega), \epsilon_{B_j}(\omega)\right) \end{array} \tag{6}$$

where

$$\Pi_1^{B_j} = \begin{pmatrix} 0 & 1 \\ 1 & 0 \end{pmatrix} \tag{7}$$

$$\Pi_2^{B_j}(\mathbf{j}\omega) = \begin{pmatrix} -J_{B_j}(\mathbf{j}\omega) & 0 \\ 0 & J_{B_j}(\mathbf{j}\omega)^{-1} \end{pmatrix} \tag{8}$$

with

$$J_{B_j}(\mathbf{j}\omega) = \Big|\sum_{k:k\in\mathcal{E}_j} L_k(\mathbf{j}\omega)\Big| + \sum_{k:k\in\mathcal{E}_j} |L_k(\mathbf{j}\omega)|\,. \tag{9}$$

- **Statement 2:** *For every $j \in \mathcal{N}$, there exist scalars $\delta_{j1}(\omega) \geq 0$, $\delta_{j2}(\omega) \geq 0$, $\delta_{j3}(\omega) \geq 0$ and $\epsilon_{G_j}(\omega) > 0$ and scalars $\Pi_{11}^k(\mathbf{j}\omega) = (\Pi_{11}^k(\mathbf{j}\omega))^* \leq 0$, $\Pi_{12}^k(\mathbf{j}\omega)$ and $\Pi_{22}^k(\mathbf{j}\omega) = (\Pi_{22}^k(\mathbf{j}\omega))^* \geq 0$, with $k = 1, \cdots, n_\ell$, satisfying $-\Pi_{12}^k(\mathbf{j}\omega) - \Pi_{12}^k(\mathbf{j}\omega)^* + 2\;\Pi_{22}^k(\mathbf{j}\omega) \leq 0$, such that*

$$\begin{array}{l} G_j(\mathbf{j}\omega) \in \mathbf{QC}\left(\delta_{j1}(\omega)\Pi_1^{G_j} + \delta_{j2}(\omega)\Pi_2^{G_j} + \cdots \right. \\ \qquad \left. \cdots + \delta_{j3}(\omega)\Pi_3^{G_j}(\mathbf{j}\omega), \epsilon_{G_j}(\omega)\right) \end{array} \tag{10}$$

where $G_j(\mathbf{j}\omega) = (\oplus_{k=1}^{n_\ell} L_k(\mathbf{j}\omega))\;(a_j^r)^T\;B_j(\mathbf{j}\omega)\;a_j^r$ and

$$\Pi_1^{G_j} = \begin{pmatrix} 0 & I_{n_\ell} \\ I_{n_\ell} & 0 \end{pmatrix} \tag{11}$$

$$\Pi_2^{G_j} = \begin{pmatrix} -2I_{n_\ell} & 0 \\ 0 & 2^{-1}I_{n_\ell} \end{pmatrix} \tag{12}$$

$$\Pi_3^{G_j}(\mathbf{j}\omega) = \begin{pmatrix} \oplus_{k=1}^{n_\ell}\Pi_{11}^k(\mathbf{j}\omega) & \oplus_{k=1}^{n_\ell}\Pi_{12}^k(\mathbf{j}\omega) \\ \oplus_{k=1}^{n_\ell}\Pi_{12}^k(\mathbf{j}\omega)^* & \oplus_{k=1}^{n_\ell}\Pi_{22}^k(\mathbf{j}\omega) \end{pmatrix}. \tag{13}$$

Proof *The complete proof can be found in [9]. A main feature of the proof is that it uses a homotopy argument to combine different conditions that have been derived for locally defined subsystems in two different network decompositions.*

Remark 1 (Microgrid decomposition) *The stability conditions in Statement 1 and Statement 2 are decentralized conditions that depend on local bus/line dynamics. They are obtained using two different decompositions of the microgrid that lead to appropriate graph separation arguments [10]. In particular, Statement 1 is derived by means of the conventional microgrid decomposition into buses and lines. Statement 2 on the other hand is based on a different decomposition of the microgrid, analogous to the one used in [8, 10], that leads to subsystems G_j involving each bus B_j and the lines L_k connected to it as follows from the sparsity structure of a_j^r.*

Remark 2 (Passivity and small-gain conditions) *The different conditions of Statement 1 and Statement 2 can be related to the usual passivity and small-gain conditions. In*

particular, in Statement 1, having $\gamma_{j2}(\omega) = 0$ in (6) *allows to recover the usual bus B_j passivity conditions while choosing $\gamma_{j1}(\omega) = 0$ allows to recover a small-gain condition on each bus B_j scaled by J_{B_j}, where the latter depends on the neighbouring line dynamics L_k. For Statement 2, we can have similar interpretations as earlier but on systems G_j this time. For instance, choosing $\delta_{j2}(\omega) = 0$ and $\delta_{j3}(\omega) = 0$ in* (10) *allows to have a passivity condition on G_j while having $\delta_{j1}(\omega) = 0$ and $\delta_{j3}(\omega) = 0$ allows to recover a small-gain condition on G_j. Finally, it is worth mentioning that in contrast to the passivity condition in Statement 1, the third component in* (10) *obtained with $\delta_{j1}(\omega) = 0$ and $\delta_{j2}(\omega) = 0$ allows to take into account the dynamics of the lines as each Π^k can be associated to each L_k.*

Remark 3 (Conservatism) *Condition* (6) *allows to combine passivity with small-gain conditions (see Remark 2), thus reducing the conservatism of more conventional passivity based results often used in the literature. Conditions* (6) *and* (10) *allow to reduce the conservatism by combining passivity with small-gain conditions but also with other conditions able to take into account the line dynamics (see Remark 2). Note that when considered individually, neither Statement 1 nor Statement 2 is less conservative compared to the other. For instance, Statement 1 considers the more commonly used bus/line decomposition and* (7) *and does not take into account the 'strength' of coupling among the bus dynamics at each frequency. On the other hand, even though Statement 2 allows to consider this coupling, it may not always hold when the couplings are too strong. Hence each statement has its own merits and a main contribution of Theorem 1 is to show that conditions* (6) *and* (10) *can be combined together pointwise over frequency by an appropriate homotopy argument (see proof in [9]), thus reducing the conservatism associated with these decentralized conditions.*

Remark 4 (Control design) *The stability conditions stated in Theorem 1 can be used as design protocols for the microgrid that need to be decided a priori, i.e. local design rules at each bus which if satisfied ensures stability of a general network. An approach when choosing such rules is to consider different conditions in different frequency ranges. For instance, the passivity conditions can be used in regimes of higher gains as passivity holds for arbitrarily large gains while small-gain conditions, or conditions that take into account the strength of the coupling, can be considered in regimes with weaker coupling and potential phase lags. It should be noted that, the generalized KYP Lemma [11] can be used to verify if the different required properties are satisfied in the corresponding frequency ranges.*

IV. Examples

To demonstrate the applicability of our results, we consider two generic examples of DC microgrids where each bus contains a controlled DC-DC converter connected to loads, see for instance [12, 13].

In particular, we will consider configurations with parameters that have been chosen in the literature in a centralized way to have good performance. We will then investigate whether stability can also be verified via the decentralized conditions derived in the paper. The significance of the latter is that they can be used as a decentralized design protocol for the network; i.e. the choice of frequency ranges where the different statements in Theorem 1 are applied and the corresponding multipliers ($\Pi_i^{B_j}$ and $\Pi_i^{G_j}$), can be used as local design rules for the converters through which stability of the network can be guaranteed.

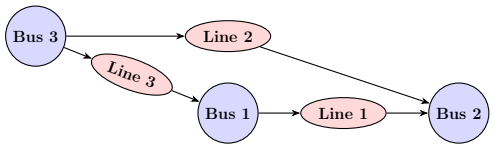

Fig. 2: Simplified representation of the considered microgrid.

In our analysis we will start with Statement 1, i.e. the bus/line decomposition, and consider first the more commonly used bus passivity condition $B_j(\mathbf{j}\omega) \in \mathbf{QC}(\Pi_1^{B_j}, \epsilon_{B_j}(\omega))$. If this condition is not satisfied for all/some frequencies, we test the small-gain condition $B_j(\mathbf{j}\omega) \in \mathbf{QC}(\Pi_2^{B_j}(\mathbf{j}\omega), \epsilon_{B_j}(\omega))$ at those frequencies. If the previous condition is also not satisfied at all/some of those frequencies, we make use of Statement 2 and we test if $G_j(\mathbf{j}\omega) \in \mathbf{QC}(\Pi_1^{G_j}, \epsilon_{G_j}(\omega))$. If the previous condition is still not satisfied at those frequencies, we test $G_j(\mathbf{j}\omega) \in \mathbf{QC}(\Pi_2^{G_j}, \epsilon_{G_j}(\omega))$ and we continue, if necessary, by testing whether $G_j(\mathbf{j}\omega) \in \mathbf{QC}(\Pi_3^{G_j}(\mathbf{j}\omega), \epsilon_{G_j}(\omega))$ can be satisfied for some choice of multipliers $\Pi_3^{G_j}(\mathbf{j}\omega)$.

The examples we are considering deal with two common situations.

- Microgrid with resistive loads where adjusting the converter control parameters to passivate the bus dynamics can result in a significant voltage deviation from the nominal value.
- Microgrid with ZIP loads dominated by their constant power components which can pose stability challenges.

Note that the numerical values used in these two examples are taken from [14, 15].

The microgrid under consideration is composed of three buses as illustrated in Fig. 2 where each bus is composed of a controlled buck converter connected to a load.

The dynamics of each bus are given by

$$\begin{cases} \dfrac{\mathrm{d}i_j(t)}{\mathrm{d}t} = \dfrac{1}{L_j}\left(-v_{B_j}(t) - R_j i_j(t) + u_j(t)\right) \\ \dfrac{\mathrm{d}v_{B_j}(t)}{\mathrm{d}t} = \dfrac{1}{C_j}\left(i_j(t) - i_{\mathrm{Load}_j}(t) + i_{B_j}(t)\right) \end{cases} \tag{14}$$

where $i_j(t)$ is the bus internal current (the inductor current), $i_{B_j}(t)$ is the bus injection current from the network, $v_{B_j}(t)$ is the bus output voltage and $u_j(t)$ is the control input of the buck converter. R_j, L_j and C_j are bus filter resistance, inductance and capacitance respectively. The control input $u_j(t)$ is given as the output of a double PI controller with the

following model, where $x_{K_j}(t)$ is the controller state vector

$$\begin{cases} \dfrac{\mathrm{d}x_{K_j}(t)}{\mathrm{d}t} = \begin{pmatrix} 0 & 0 \\ K_{I_{v_j}} & 0 \end{pmatrix} x_{K_j}(t) + \begin{pmatrix} 1 & 0 \\ K_{P_{v_j}} & -1 \end{pmatrix} \begin{pmatrix} e_{v_j}(t) \\ i_{L_j}(t) \end{pmatrix} \\ u_j(t) = \begin{pmatrix} K_{P_{i_{L_j}}} K_{I_{v_j}} & K_{I_{i_{L_j}}} \end{pmatrix} x_{K_j}(t) + \dots \\ \qquad \dots + \begin{pmatrix} K_{P_{i_{L_j}}} K_{P_{v_j}} & -K_{P_{i_{L_j}}} \end{pmatrix} \begin{pmatrix} e_{v_j}(t) \\ i_{L_j}(t) \end{pmatrix} \end{cases}$$

The gains $K_{P_{v_j}}$ and $K_{I_{v_j}}$ are the proportional and the integral gains, respectively, of the voltage PI controller (outer controller) while $K_{P_{i_j}}$ and $K_{I_{i_j}}$ are those of the current PI controller (inner controller). The signal $e_{v_j}(t)$ is the voltage tracking error given by $e_{v_j}(t) = v_{r_j}(t) - v_{B_j}(t)$ where $v_{r_j}(t)$ is the desired bus output voltage which is adjusted according to $i_{B_j}(t)$ such that $v_{r_j}(t) = v_{r_{\text{nom}}} + R_{\text{droop}_j} i_{B_j}(t)$ with $v_{r_{\text{nom}}}$ the nominal voltage and R_{droop_j} the droop coefficient.

The current $i_{\text{Load}_j}(t)$ in (14) is the load current and its expression depends on the load type as it will be shown in the two cases below.

A. Microgrid with resistive loads

In this case, each bus is connected to a resistive load $R_{\text{Load}_j} > 0$ and $i_{\text{Load}_j}(t)$ is given by

$$i_{\text{Load}_j}(t) = R^{-1}_{\text{Load}_j} v_j(t).$$

To investigate the stability of this microgrid, we start with the usual passivity argument of Statement 1 corresponding to $B_j(\mathbf{j}\omega) \in \mathbf{QC}(\Pi_1^{B_j}, \epsilon_{B_j}(\omega))$. The analysis reveals that the different buses are not passive over all frequencies especially at high frequencies as it can be seen in Fig. 3(a).

A common approach to enhance bus passivity is to increase the droop coefficients R_{droop_j} until we have $B_j(\mathbf{j}\omega) \in \mathbf{QC}(\Pi_1^{B_j}, \epsilon_{B_j}(\omega))$ at all frequencies. However, the consequence will be an important output voltage deviation from the nominal value $v_{r_{\text{nom}}}$ which makes this approach non practical for the operation of the microgrid.

To go beyond the passivity condition using Statement 1, we investigate if the small-gain condition $B_j(\mathbf{j}\omega) \in \mathbf{QC}(\Pi_2^{B_j}(\mathbf{j}\omega), \epsilon_{B_j}(\omega))$ is satisfied at least at high frequencies. The results presented in Fig. 3(b) affirm that the latter condition is satisfied at high frequencies where passivity failed. Hence, the microgrid of Fig. 2 with resistive loads is stable since Statement 1 is always satisfied at each frequency $\omega \in \overline{\mathbf{R}}_+$ as it can be seen in Fig. 3(c).

Therefore, a scalable control protocol when considering such microgrids in a general network topology can be to require the dynamics at each bus to satisfy

- $B_j(\mathbf{j}\omega) \in \mathbf{QC}(\Pi_1^{B_j}, \epsilon_{B_j}(\omega))$ at a prescribed low frequency range $\omega < \omega_c$.
- $B_j(\mathbf{j}\omega) \in \mathbf{QC}(\Pi_2^{B_j}(\mathbf{j}\omega), \epsilon_{B_j}(\omega))$ at higher frequencies $\omega \geq \omega_c$.

B. Microgrid with ZIP loads

We consider now the case where the loads are not just resistive and they also contain constant current and constant power elements. The load current $i_{\text{Load}_j}(t)$ becomes

$$i_{\text{Load}_j}(t) = \bar{i}_{\text{Load}_j} + Z^{-1}_{\text{Load}_j} v_{B_j}(t) + P_{\text{Load}_j} v_j^{-1}(t)$$

where $\bar{i}_{\text{Load}_j}$, $Z_{\text{Load}_j} = R_{\text{Load}_j} > 0$ and $P_{\text{Load}_j} > 0$ are the current, impedance and power of the constant current load, the constant impedance load and the constant power load respectively.

The presence of constant power loads has a destabilizing effect on the bus dynamics since they behave as negative resistance elements. To guarantee bus stability using a passivity argument, we require that at steady state, the effect of the constant impedance loads is larger than that of the constant power loads [16, 17], that is

$$Z^{-1}_{\text{Load}_j} v_{r_j}(t) > P_{\text{Load}_j} v_{r_j}^{-1}(t).$$

If the previous condition is satisfied, then it is possible to certify the stability of the microgrid with ZIP loads using Statement 1 in a similar way to the case of resistive loads presented earlier. Nevertheless, in many practical cases, the constant power loads can be larger than the constant impedance loads. In this case, Statement 1 alone will not be able to certify microgrid stability as it can be seen in Fig. 4(a). Note that in contrast to the case of resistive loads, the passivity condition does not hold at low frequencies while

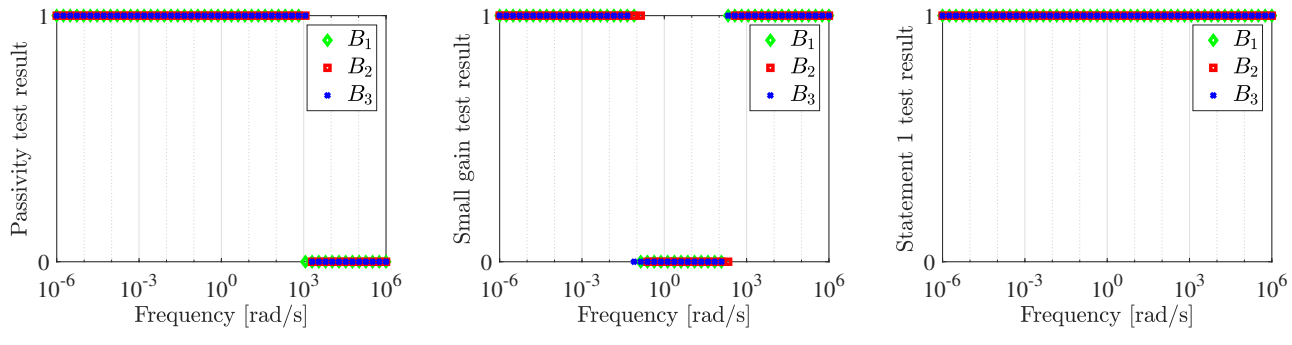

(a) (b) (c)

Fig. 3: Stability assessment results of the microgrid of Fig. 2 with resistive loads using: (a) passivity, (b) small gain and (c) Statement 1 (passivity and small gain). Note that at each frequency, a value at 0 on the vertical axis means that the considered test has failed while 1 means it has passed.

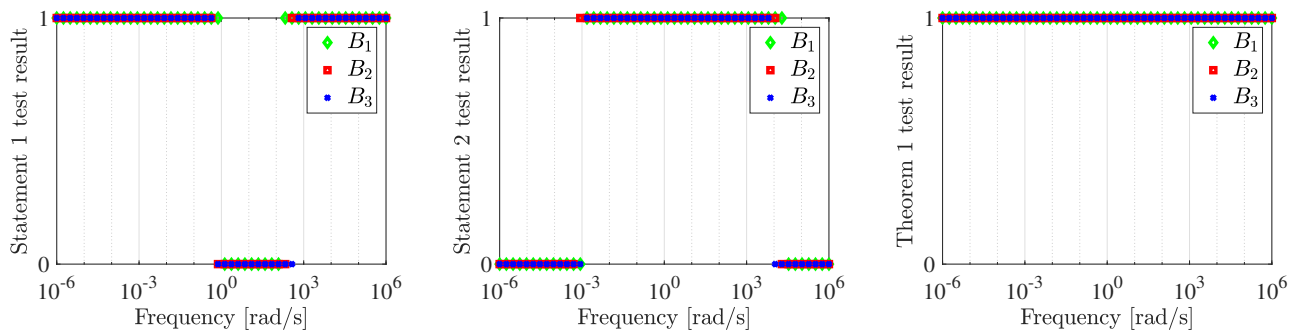

(a) (b) (c)

Fig. 4: Stability assessment results of the microgrid of Fig. 2 with ZIP loads where $P_{\text{Load}_j} v_{r_j}^{-1}(t) > Z_{\text{Load}_j}^{-1} v_{r_j}(t)$ using: (a) Statement 1, (b) Statement 2 and (c) Theorem 1. Again note that at each frequency, a value at 0 on the vertical axis means that the considered test has failed while 1 means it has passed.

the small-gain condition holds. Note also that none of these conditions hold in medium frequencies, see Fig. 4(a).

Statement 2 allows to go beyond passivity and small-gain conditions of the conventional bus/line microgrid decomposition. In fact, the analysis reveals that by considering the small-gain condition in the new decomposition $G_j(\mathbf{j}\omega) \in \mathbf{QC}(\Pi_2^{G_j}, \epsilon_{G_j}(\omega))$, Statement 2 is satisfied at medium frequencies where Statement 1 failed, see Fig. 4(b). Therefore, we have Statement 1 and/or Statement 2 satisfied at each frequency $\omega \in \overline{\mathbf{R}}_+$ as it can be seen in Fig. 4(c), and hence the microgrid of Fig. 2 with ZIP loads considered (dominated by constant power loads) is stable.

To conclude, when considering such microgrids in a general network topology, a scalable control protocol is to design controllers able to satisfy

- $B_j(\mathbf{j}\omega) \in \mathbf{QC}(\Pi_2^{B_j}(\mathbf{j}\omega), \epsilon_{B_j}(\omega))$ in a prescribed low frequency range.
- $G_j(\mathbf{j}\omega) \in \mathbf{QC}(\Pi_2^{G_j}, \epsilon_{G_j}(\omega))$ in a prescribed medium frequency range.
- $B_j(\mathbf{j}\omega) \in \mathbf{QC}(\Pi_1^{B_j}, \epsilon_{B_j}(\omega))$ at high frequencies.

V. Conclusions

We have derived decentralized stability conditions for DC microgrids. Our analysis takes into account the line dynamics and also allows higher order models for the DC-DC converters at each bus. By exploiting various decompositions of the network, we have derived multiple decentralized input-output stability conditions that also allow to exploit the coupling of each bus with neighboring lines. We have used appropriate homotopy arguments to combine these conditions pointwise over frequency thus reducing the conservatism in the analysis. The efficiency of the obtained results has been illustrated through examples.

References

[1] J. J. Justo, F. Mwasilu, J. Lee, and J. Jung, "AC-microgrids versus DC-microgrids with distributed energy resources: A review," *Renewable and Sustainable Energy Reviews*, vol. 24, pp. 387 – 405, Aug. 2013.

[2] A. T. Elsayed, A. A. Mohamed, and O. A. Mohammed, "DC microgrids and distribution systems: An overview," *Electric Power Systems Research*, vol. 119, pp. 407 – 417, Feb. 2015.

[3] J. M. Guerrero, J. C. Vasquez, J. Matas, L. G. de Vicuna, and M. Castilla, "Hierarchical control of droop-controlled AC and DC microgrids-a general approach toward standardization," *IEEE Transactions on Industrial Electronics*, vol. 58, pp. 158–172, Jan. 2011.

[4] J. Zhao and F. Dörfler, "Distributed control and optimization in DC microgrids," *Automatica*, vol. 61, pp. 18 – 26, Nov. 2015.

[5] M. Tucci, S. Riverso, and G. Ferrari-Trecate, "Line-Independent Plug-and-Play Controllers for Voltage Stabilization in DC microgrids," *IEEE Transactions on Control Systems Technology*, vol. 26, pp. 1115–1123, May 2018.

[6] Y. Gu, W. Li, and X. He, "Passivity-based control of DC microgrid for self-disciplined stabilization," *IEEE Transactions on Power Systems*, vol. 30, pp. 2623–2632, Sept. 2015.

[7] V. Nasirian, S. Moayedi, A. Davoudi, and F. L. Lewis, "Distributed cooperative control of dc microgrids," *IEEE Transactions on Power Electronics*, vol. 30, pp. 2288–2303, Apr. 2015.

[8] K. Laib, J. Watson, and I. Lestas, "Decentralized stability conditions for inverter-based microgrids," in *2020 IEEE Conference on Decision and Control (CDC)*, pp. 1341–1346, 2020.

[9] K. Laib, J. Watson, Y. Ojo, and I. Lestas, "Decentralized stability conditions for DC microgrids: Beyond passivity approaches," *arXiv preprint arXiv:2109.02708*, 2021.

[10] I. Lestas, "On network stability, graph separation, interconnection structure and convex shells," *2011 IEEE Conference on Decision and Control (CDC)*, pp. 4257–4263, 2011.

[11] T. Iwasaki and S. Hara, "Generalized KYP lemma: Unified frequency domain inequalities with design applications," *IEEE Transactions on Automatic Control*, vol. 50, pp. 41–59, Jan. 2005.

[12] A. Bidram, V. Nasirian, A. Davoudi, and F. L. Lewis, *Cooperative Synchronization in Distributed Microgrid Control*. Springer, 2017.

[13] M. Cupelli, A. Riccobono, M. Mirz, M. Ferdowsi, and A. Monti in *Modern Control of DC-Based Power Systems*, Academic Press, 2018.

[14] X. Lu, K. Sun, J. M. Guerrero, J. C. Vasquez, L. Huang, and J. Wang, "Stability enhancement based on virtual impedance for DC microgrids with constant power loads," *IEEE Transactions on Smart Grid*, vol. 6, pp. 2770–2783, Nov. 2015.

[15] D. Zammit, C. S. Staines, M. Apap, and A. Micallef, "Paralleling of buck converters for DC microgrid operation," in *2016 International Conference on Control, Decision and Information Technologies (CoDIT)*, pp. 070–076, April 2016.

[16] M. Cucuzzella, R. Lazzari, Y. Kawano, K. C. Kosaraju, and J. M. A. Scherpen, "Robust passivity-based control of boost converters in DC microgrids," in *2019 IEEE Conference on Decision and Control (CDC)*, pp. 8435–8440, 2019.

[17] P. Nahata, R. Soloperto, M. Tucci, A. Martinelli, and G. Ferrari-Trecate, "A passivity-based approach to voltage stabilization in DC microgrids with ZIP loads," *Automatica*, vol. 113, p. 108770, Mar. 2020.